Optimization of Copper Upcast Technology For Cable Manufacturing Industry

Aram Hovhannisyan

Capstone Submitted to the College of Science & Engineering

American University of Armenia

In Partial Fulfillment of the Requirements

for the Degree of Bachelor of Science in

Engineering Sciences

Supervisor: Dr. Hrachya Kocharyan

May 2023

Acknowledgements

Firstly, I would like to express my special gratitude towards my project supervisor Dr. Hrachya Kocharyan, who not only agreed to supervise my capstone, but also constantly guided and advised me during the whole project. Dr. Kocharyan was always available for questions and discussions regarding the complex topics which were vital for the project completion. Courses like Thermodynamics and Introduction to Material Science taught by Dr. Kocharyan were the key to reaching the final goal of the project, which is the optimization of the metallurgical production process. Thank you for all the support and compassion towards me during this amazing academic journey.

I want to express my sincere thanks to "N-S" LLC for giving me the opportunity to solve their production optimization problem for newly imported machinery and for financing the project in all aspects. The knowledge and experience gained during this journey is invaluable and surely will help me in my future career.

Special thanks to Mr. Vardan Hayrapetyan and the Chemical Physics Institute of Armenia, which provided me with an X-ray diffractometer from their lab and processed the data using their software. Mr. Vardan Hayrapetyan also advised me regarding specimen preparation and testing.

I also want to thank Mr. Arman Asatryan, facilities engineer at the engineering laboratory. Mr. Asatryan advised and helped me with specimen preparation for metallographic and mechanical testing using the equipment and machinery in the lab.

My classmates and friends had significant investment in the success of my studies at AUA and in my capstone project. They not only helped me morally but also with understanding difficult engineering concepts through completion of various engineering projects assigned to us. Aleksandr Hakobyan, Gor Isoyan, Krist Samuel Siraki, Artur Ghukasyan, Arman Babayan, Elizabeth Vickery and others are wonderful people, who are all specialized in extremely diverse branches of the enormous world of engineering sciences. I wish success for all of them and hope to keep in touch with these incredible people in my professional career.

Abstract

Copper is one of the most widespread and at the same time one of the most important metals in everyday life. All of the electronic devices, machinery, vehicles, planes, trains etc. all depend on copper wires. Another critical infrastructure that almost entirely depends on copper wires is the power transportation from power generating stations to industries and end users. Although copper usage is widespread, copper wire production process is not trivial as it depends on many parameters. In the copper fabrication process, usually a larger diameter copper rod is produced, the diameter of which is later reduced to the needed diameter to form the copper wires, in a process known as wire drawing. The parameters during the copper fabrication process affect both the copper rod and later the wire drawing processes. These parameters are copper melt temperature, rod fabrication parameters, rod cooling temperature and the wire drawing parameters. In the presented experiments, the melt temperature and the cooling temperatures are remained constant, and the wire drawing is out of scope of this research. This work is concerned with the rod fabrication parameters and the optimization of those parameters. The rod fabrication parameters are the casting speed, pull distance and the interval time. These three parameters were varied within physical limits of the setup to investigate the effects of those parameters on the properties of the fabricated samples. XRD analysis and three-point bending tests were performed to investigate changes to the internal structure and the mechanical properties at various growth parameters. It was found that all three parameters have significant effect on the rod properties, and a multi-body optimization is required to find optimal parameters to maximize the production, an effort that was ordered and sponsored by “N-S LLC”.

Table of Contents

Chapter 1: Literature Review

1.1 Introduction

Heavy metallurgy evolved greatly starting from the first industrial revolution up to our days. Metal processing and casting technologies adapted for various applications and product ranges. The most widespread technologies include processes like sand casting, injection mold casting, semicontinuous and continuous casting. The latter was introduced by Sir Henry Bessemer in 1857. Bessemer applied for a patent for a technology which included two counter-rotating rollers on top of which the metal liquid is being poured. As a result of cooling and pressure from the rollers, one could acquire desired shapes of uniform continuous cast metal semi-fabricated products, ready for further processing. Since the first introduction of the above technology, it underwent various improvements and variations, most significantly the horizontal continuous casting, vertical upward casting, and vertical downward casting technologies were developed, which are shown in ***Figure 1***. Vertical semicontinuous and continuous casting technologies are most popular for producing both ferrous and non-ferrous metal rods and billets. Downward casting is a commonly used method for casting steel billets, as well as other ferrous metal billets and sheets. Vertical downward casting technology is also applied in aluminum billet semicontinuous casting which is a vital process for aluminum profile extrusion technology.

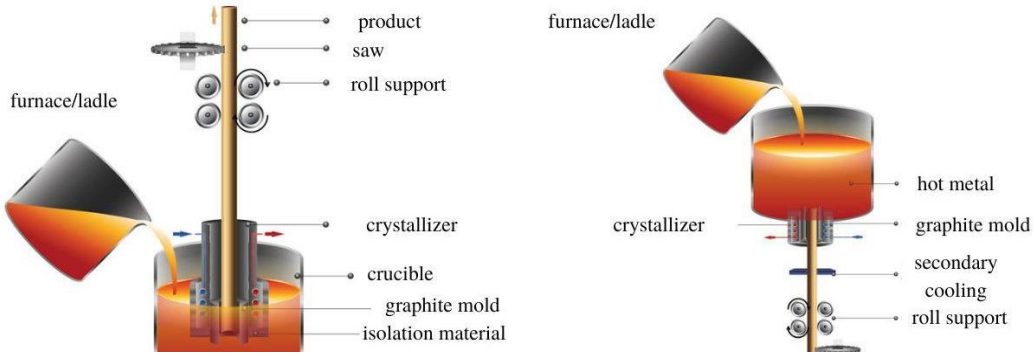

***Figure 1**: Schematic representation of (a) vertical upward, (b) vertical downward casting technologies (© "KMM Bronze", 2022)*

Application of vertical upward casting technology is production of nonferrous metal rods, particularly copper and aluminum rods, primarily used in the cable manufacturing industry.

1.1.1 Comparison of Casting Technologies

Downward casting is specifically designed for large diameter billet castings, since this technology is offering better heat extraction from the melt which ensures full solidification process for large amount of melt passing through the cooling mold. Additionally, downward casting also has the capability of casting small diameter rods and wires, even though it is not widespread. On the other hand, upward casting is specifically designed for small diameter rods and wires and is incapable of casting large billets, because of lower heat extraction capacity. It is also unreasonable to cast heavy billets upward in technological point of view. Horizontal casting technology, on the other hand, is primarily used in casting metal tubes of large diameters and is widely used in diverse industries, including cooling systems using brass or copper tubes.

After casting, copper rods/billets undergo further processing either by wire drawing process for rods and wires, or extrusion process for billets. For wire drawing process, vertical upward continuous casting technology offers highest quality in terms of copper rod microstructure, which is crucial during the procedure, as in case of any significant defect in the crystal structure of the metal, wire breakage occurs, leading to significant delay and cost inefficiency in the whole manufacturing process. Moreover, the quality of the product can also be affected, and those products may not pass the set requirements, as power cables have strict safety and quality standards to correspond to.

For the above reasons, in the last decade, upward continuous casting technology has taken over the power cable manufacturing sector. The microstructure of the copper rod obtained by the above method is mainly dependent on several parameters, namely the purity of the raw material, cooling water flow rate, its temperature, casting parameters, superheat modulus, oxygen content in the cast material etc. Deviation from any of the above parameters may lead to poor copper rod production efficiency and quality, henceforth it is vital to set correct parameters to avoid delays in the production and maximize its quality. Research and experiments are conducted in collaboration with “N-S LLC” specialized in copper and aluminum cable manufacturing in Abovyan, Armenia. Company provided their induction heating copper upward casting furnace for the experimental

part of the research. The aim of this study is the optimization of copper upward casting technology by studying the optimal parameter sets for copper rods and wires used in the cable manufacturing industry.

1.2 Copper Crystal Structure

Copper is one of the oldest metals known to humankind. From ancient times, to nowadays, copper plays a significant role in various industries, such as heating and cooling systems, electrical power transmission lines, microelectronics, pipelines, roofing, industries with highly corrosive environments etc. The reason is that copper has outstanding mechanical, thermal, electrical properties, while being significantly more widespread, easy to mine and less costly than any other metal with similar property sets. Copper can be described as a tough, ductile, and malleable material, ideal for tube forming hot rolling and wire drawing processes. It also features great heat conductivity and high electrical conductivity.

1.2.1 Copper Crystal Structure: Crystalline and Amorphous Solids

Two main groups are defined for solid materials, namely crystalline solids**,** and amorphous solids [1]**.** Crystalline solids are composed of strictly defined microstructure, meaning, the atoms inside the solid are located so that they all acquire specific lattice structure. Most of the metals are crystalline solids and can be found predominantly in three crystal structures, which are face centered cubic (FCC), body centered cubic (BCC), and hexagonal close packed (HCP) structures [1]. Schematic representation of FCC and BCC lattice structures is presented in ***Figure 2***. In most cases, the lattice structure of metals is dependent on the alloy type. Since the material of interest of this study is pure copper cathode (purity above 99.99%), which features an FCC crystal structure [9], HCP and BCC structures will not be further considered.

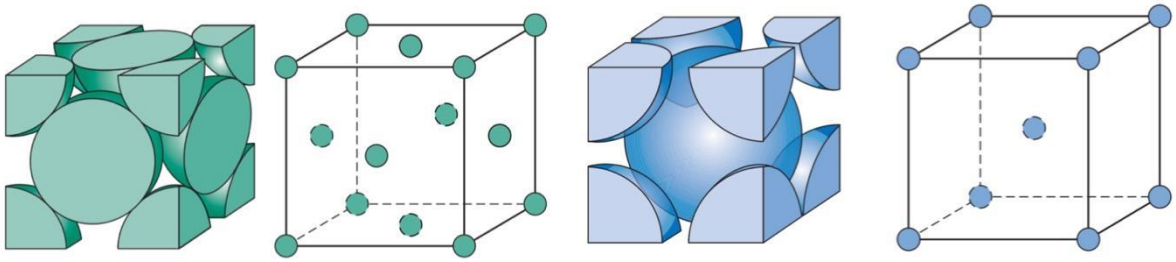

(a) ***(b)***

Figure 2*: Schematic representation of (a) FCC and (b) BCC crystal structures [1]*

Amorphous structures, on the other hand, have no systematic and predictable arrangement of their atoms. Furthermore, many amorphous solids tend to flow at an extremely slow rate, which makes them more similar to liquids rather than to solids, hence these non-crystalline materials are often referred as supercooled liquids. Most ordinary examples of amorphous solids are glasses, polymers, rubbers etc. Polymers like polyethylene and polyvinylchloride are also widely used in cable manufacturing industry for their outstanding thermal, mechanical, and electrical insulating properties.

1.3 Copper Power Cables

Power cable production is a complex and multidisciplinary production cycle, with various processes involved in it. Additionally, power cables differ by their structure, application and most significantly their quality. For the specific matter, classifications and production cycles used in power cable production are discussed below.

1.3.1 Power Cable Types

Considering that the current research is strongly related to the cable manufacturing process, a vital aspect to be defined is the power cable categories, types and classes and corresponding manufacturing processes behind those products. The power cable definition is blurred since diverse sources bring up unique parameters which are meant to distinguish between wires and power

cables. The main constraints, however, are that power cables are composed of one or several insulated conductor cores, inside a metallic or nonmetallic sheath, which in turn, may be composed of a protective sleeve usually composed of specific polymer or resin, which may, in turn, contain a metallic armor and additional protective sleeve [3]. Yet the constraints are often changed according to the unique requirements. Power cable usage is extremely widespread in every aspect of the modern world, and accordingly, dozens of categories were designed to meet every possible use case. The structure of any power cable is mainly dependent on the use case and the load capacity it can be subjected to. In this context, cables are classified in four major groups, namely, stationary power cables for up to 1000V, flexible power cables for up to 1000V (low voltage), stationary power cables for up to 35kV (medium voltage) and stationary power cables for up to 110kV (high voltage) [2]. Each of the above power cable types has a unique production cycle, yet the current study is only focused on the first two categories, which are stationary and flexible power cables for up to 1000V, because of the scarce availability and structural complexity of the other two types of power cables.

1.3.2 Power Cable Flexibility Classes

Another vital aspect for power cables is the flexibility class of the conductor. According to the IEC60228 standard, there are four major flexibility classes for cable conductors [8]. Class 1 conductors are composed of a single solid core conductor while class 2 conductors are composed of minimum of 7 stranded and coaxially twisted wires. The above-mentioned classes are designed for fixed or stationary use. Class 5 and 6 conductors are classified by maximum diameter of the stranded conductors. These values differ according to a given cross sectional area of the power cable which may range from $0.5mm^2$ and up to $630mm^2$ according to the same standard [8]. Class 5 (flexible conductor) and class 6 (extra flexible conductor) are used in non-stationary use, such as overhead power transmission and elevator power supply where high flexibility of power cables is required. It is also necessary to note that class 5 and class 6 power cables have higher net electrical resistance per kilometer length in comparison to class 1 and class 2 conductors. Even though in most use cases the resistance difference may be neglected, in some error sensitive cases the difference should be considered.

1.4 Copper Power Cable Manufacturing Process

1.4.1 Production of Copper Rod

Production cycle for power transmission cables and wires is composed of several steps starting from the raw material processing to semi-fabricated products and up to finished power cables. Current study focuses on the first step in this complicated process, which is production of the copper rod by means of copper casting technologies discussed earlier. Three known processes for copper continuous casting were presented in the introduction. It was also stated that vertical casting processes are the best choices for copper cable production. The raw material, pure copper cathode plate with relatively small amount of copper scrap is put in the induction melting chamber where the metal is heated until a uniform liquid phase of the metal is reached. The metal is then poured in a silicon carbide crucible where the casting process is conducted, using tube shaped graphite molds of different diameters, according to corresponding product. The process has significant importance in the whole power cable production cycle since any deviation from acceptable standards may affect the further processing and even lead to defective product. The main factors that can help avoid such circumstances is the melting and casting parameter optimization, which the current study intends to provide.

1.4.2 Wire Drawing Process

The next production process in power cable manufacturing is the wire drawing process. The copper rod from the first process is passed for further processing using special wire drawing machinery and special polycrystalline dies passing through which the initial rod stretches axially and decreases in diameter to a specific size according to IEC60228 standard [8]. Standard wire drawing machines usually feature a set of drawing dies consisting of 11 or 13 dies and pairs of capstan drums corresponding to each drawing die [3]. After passing each die, because of elongation of the copper wire, the speed of the wire section that passed the drawing die is significantly higher than of the section that is yet to pass the same die.

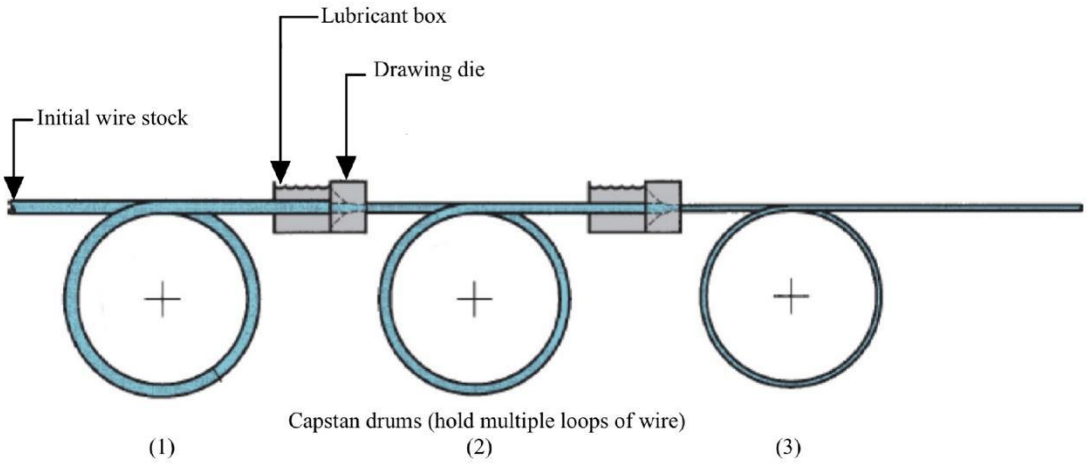

***Figure 4**: Schematic representation of the copper wire drawing process*

Copper is known to undergo a process called strain hardening, or work hardening [1], [13]. Metals that undergo work hardening transition from being relatively more ductile to becoming harder and stronger as a result of plastic deformation. Metals that are known to undergo work hardening are steel, brass, copper, aluminum, precious metals such as gold [1]. This work hardening can be desired in some cases, for example in production of various steel tools, or in wearable jewelry, but it can also be undesirable, for example aircrafts have a limited lifetime, because the aluminum structures can undergo work hardening over time and become unsafe at some point. The work hardening is undesirable in copper wire production as well, especially if flexibility is important. As it was already mentioned above, the as-produced copper rods should undergo a wire drawing process. Wire drawing process can be viewed as a work hardening process, which will result in hardening of the copper rods. If copper rod is already hard before work hardening, the wire drawing process can become a difficult or even impossible task. Hence, it is desirable to have somewhat softer copper rods before starting the wire drawing process. Often, it is needed to extensively reduce the diameter of the rod, which can be done in one of in a few steps. As a result of trying to achieve wire drawing in one step, tension in the wire increases which can eventually lead to wire breakage. To avoid that, capstan drums of varying diameters are used in a

multi-stage wire drawing process to lower the effect of the tension in the wire and to avoid the wire failure. Unfortunately, this multi-stage wire drawing negatively affects the speed of wire production, but it is impossible to avoid it. High friction between the drawing die and the wire is another challenge during the above process since it generates large amount of heat to the wire and the dies, hence the drawing machines are also equipped with lubricant boxes, which lubricate the components and operate as a coolant for both the dies and the wire (Figure 4). After the process, the initial copper rod of diameter 8mm may either reach to diameter of 1.78mm or be drawn until reaching a diameter of 0.38mm. This further processing is applicable for cases where class 5 or class 6 power cables are to be produced. The key parameters such as elongation percentage and tensile strength are the key for this process to be continuous and to avoid any waste in the production cycle. After the above processes, copper wire might undergo wire twisting process. This process is only applicable for Class 2, Class 5, and Class 6 power cables where multiple wires exist in a single conductor core.

1.4.3 Copper Wire Twisting Process

The wire twisting process is insignificantly different for different cables. The only difference is in the input number of coils which are drawn into the main chamber where all the wires are being intertwisted to be transformed to a single extra flexible core of corresponding class. The number of feeding coils is equal to the number of the wires in the core which corresponds to IEC60228 standard.

1.4.4 Insulative Layer Extrusion on Bare Conductor Core

Polymers, such as, polyvinylchloride (PVC), low density polyethylene (LDPE), high density polyethylene (HDPE) and cross-linked polyethylene (XLPE) are the most common amorphous materials with good insulative properties which are widely used in cable manufacturing processes [3]. Besides, being insulators, these materials are relatively lightweight, flexible, and extremely durable. Even though all the above-mentioned polymers feature unique parameter sets, and are used in different cases, the process of covering the bare conductor core with the protective sleeve is identical for all of them. The polymer granules are fed to a special chamber from where the granules are moved by a transporting screw through a cylindrical heating unit where the melting of the polymer takes place. The screw also mixes the polymer melt until it becomes

uniform and is ready for the extrusion process. After uniform molten polymer is ready, it is pressed through special tube-shaped extrusion die where the polymer is uniformly covering the copper conductor surface. The process is repeated until corresponding standard for the cable is reached. After cooling the power cable is passing the quality tests in the laboratory environment and after passing the test it is ready for exploiting.

1.5 Aim of the Study

The current work is sponsored by "N-S LLC" to optimize their copper-wire production technology. Current study focuses on the casting parameter set optimization for upward casting technology for a mass production. The aim is to provide technology users with optimal parameters such as casting speed, pull distance and interval time (will be explained in the next chapter), which can provide maximum productivity while also offering the most optimal mechanical and electrical properties for processing those copper rods.

Chapter 2: Experimental Setup and Procedure

2.1 Experimental Setup and Consumables

Casting process is conducted using the Continuous Casting machinery provided by "N-S" LLC with medium frequency (8KHz) induction heating system having total generator power of 70 kWh and with loading capacity of 100kg of copper. Casting machine consists of heating unit, primary cooler or crystallizer, servo motor-based withdrawal unit and coiler. Crystallizer assembly consists of steel heat exchanger with embedded water inlet and outlet, graphite mold of inner diameter of 8mm, which is partially submerged in the copper melt and is covered by graphite protective jacket (***Figure 5)***. Induction heating unit features electromagnetic steering functionality, meaning, the melt in the machine constantly moves from bottom to the surface enabling more uniform melt temperature. Continuous casting machine also features a temperature regulation control unit with K-type thermocouple equipped with silicon carbide protective sleeve for long term melt measurements. Use of conventional thermocouples with steel protective sleeves results in gradual degrading of the steel sleeve and henceforth leads to thermocouple failure.

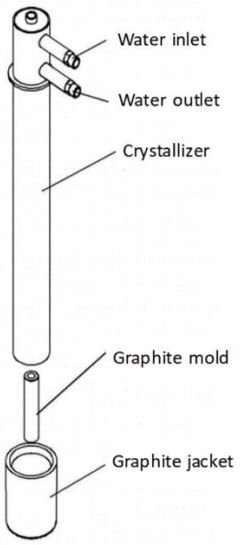

Figure 5*: Crystallizer Assembly*

Durable silicon carbide ceramic crucible (SiC) with 100kg load capacity is being used for melting and casting. As opposed to its graphite alternative SiC crucible is more inert to the copper melt as graphite crucibles gradually decay when in reaction with copper melt. This process of crucible's decay has two advantages over SiC analogues. Firstly, it releases most of gases present in the copper melt and stabilizes the melt. Secondly, usage of graphite crucible during casting process prevents metal oxidation, a common issue during any metal casting process. For this specific reason, SiC crucibles are used along with graphite powder which is being poured on the surface of the copper melt. Graphite powder in this case acts like a substitution to the graphite crucible and features the same degassing and antioxidation properties. Furthermore, coverage of

the surface of the melt results in better thermal isolation of the system, meaning melt temperature will be less vulnerable to external conditions.

2.2 Experimental Procedure: Casting Process and Parameters

Continuous Casting process begins with loading the machine with extra high purity cathode copper (above 99.50%) material and small amount of copper cable scrap in the crucible. After loading, copper is heated until it reaches its liquidus temperature of 1085°C. At this point copper melt is releasing its internal gases, most significantly hydrogen, henceforth it is vital to pour graphite powder with degassing properties into the melt before proceeding to casting procedure. Graphite powder, along with magnetic steering feature of the machine, releases internal gases from the melt, prevents further oxidation and acts as a thermal insulation layer helping to maintain constant melt temperature throughout the experiment. After degassing process, the next step is to add constant superheat of 66°C, so that the net temperature of the melt becomes 1151°C with a constant deviation of $\pm$ 2°C. This parameter will remain constant throughout the experiment for all cast rod samples. Adding superheat is vital to reach minimum possible viscosity to ensure constant flow of copper melt in the cooling mold. Overall, all parameters vital of successful casting process are as follows:

- Cooling water flow rate
- Cooling water temperature
- Casting Speed
- Pull distance
- Pause time
- Superheat size

Casting machine used in the experiments adopts intermittent extraction with pause technique, meaning rod is withdrawn to certain height, then withdrawal stops for given amount of time and the cycle repeats. Casting parameters i.e., casting speed, pull distance and pause time are set from the control panel of the machine where casting speed sets the linear speed of withdrawal of the rod, pull distance sets the step height before the withdrawal is paused and pause time sets the time when the cycle will repeat itself. ***Figure 6*** shows schematic representation of the

withdrawal cycle. As it can be seen, the pulling process is not completely constant, and casting speed has some acceleration and deceleration ranges, but for simplicity, we will assume a constant casting speed.

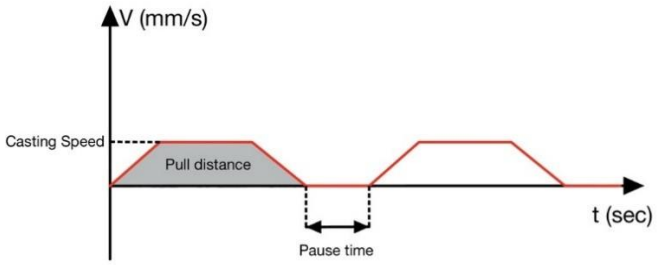

***Figure 6**: Withdrawal cycle of the casting machine*

Through the experiment, cooling water temperature was held at a constant value of 25°C, and the water flow rate was 25 liters per minute. The effect of cooling temperature on the properties of the copper rod are of interest as well, however, the experiments would be too complicated and too expensive to conduct, hence it was decided to maintain a constant cooling temperature. Variable parameters, used during the experiment are casting speed, pull distance and interval time of the withdrawal cycle. In total, 10 different cast samples were prepared, with parameters presented in ***Table 1.***

Sample	Pull Distance (mm)	Interval Time (s)	Casting Speed (mm/sec)	Melt Temperature (C°)	Water Flow Rate (liters/min)	Casting Mold	Rod diameter (mm)
Cast 1	11	0.5	21	1150	25	Graphite	8mm
Cast 2			44				
Cast 3			66				
Cast 4			88				
Cast 5	6,5	0.5	44				
Cast 6	15						
Cast 7	24						
Cast 8	11	0.1	44				
Cast 9		0.3					
Cast 10		1					

***Table 1:** Samples cast in the experiment, with the corresponding casting parameters changed*

2.2.1 Metallography

The crystalline structure of the casted copper rods was characterized by X-ray diffraction (XRD) analysis at Institute of Chemical Physics (NAS RA) using MiniFlex benchtop X-ray diffractometer equipped with CuKα (λ=0.154 nm) X-ray source (40 kV, 40 mA) in Bragg Brentano geometry. In the XRD measurements, the X-rays are generated by a cathode ray tube, filtered to get a monochromatic radiation, concentrated and directed towards the sample. The interaction of X-rays and the sample produces constructive interference when the Bragg's law is satisfied. By scanning a wide range of angles, all diffraction directions can be determined. Using XRD studies, it is possible to identify the crystalline structure and phases of the material, determining the crystallite sizes and orientations as well as atomic arrangements etc.

The average crystallite size was estimated from the XRD spectra using Scherrer formula [1]:

$$D = \frac{k\lambda}{\beta cos\theta} \tag{2.1}$$

where D is the average crystallite size in nanometers (nm), K=0.9 is the shape factor, λ=0.154 nm is the wavelength of the x-ray radiation, β is the full width at half-maximum (FWHM) of the preferred peak in radians (rad), θ is the diffraction angle in radians (rad).

The interplanar spacing of the diffraction pattern was calculated using the Bragg's law given as [10]:

$$d = \frac{n\lambda}{2sin\theta} \tag{2.2}$$

where d is the inter planar spacing in nanometers (nm), n=1 is the order of diffraction.

The lattice constants of the experimental films were evaluated using the d-spacing formula for FCC structure [10]:

$$\frac{1}{d^2} = \frac{h^2 + k^2 + l^2}{a^2} \tag{2.3}$$

where h, k, l are Miller indices and a is the lattice constant.

2.2.2 Mechanical Testing

Mechanical properties, namely Young's modulus of the specimen were tested using the three-point bending technique as shown in ***Figure 7***. The method allows to calculate the flexural elastic modulus as the slope of flexural stress vs flexural strain curve of each specimen under a perpendicular to the specimen load. While performing a tensile experiment to find the Young's modulus is a more preferred technique, due to technical limitations such as copper demanding more capable load cells, as well as the round shape of the samples, we had to resort to using a three-point bending test. However, flexural modulus is equal to regular Young's modulus in isotropic materials, like copper and most of other metals. Flexural strength of a round specimen can be evaluated using the following equation [1]:

$$E = \frac{FL^3}{12\pi\delta r^4} \tag{2.4}$$

where E is the flexural strength in megapascals, F is the force applied, L is the length of the specimen, δ is the maximum deflection of the beam from the initial position under the load and r is the radius of the specimen. Due to technical limitation, the three-point bending was performed using in-house built setup, where the force was applied by gravity of a known mass, and the deflection was calculated using a micrometer. For the evaluation of the flexural strength, the following standard values were taken. Mass was taken to be 1.1kg, length was 230mm and radius of the rod was equal to 3.75mm.

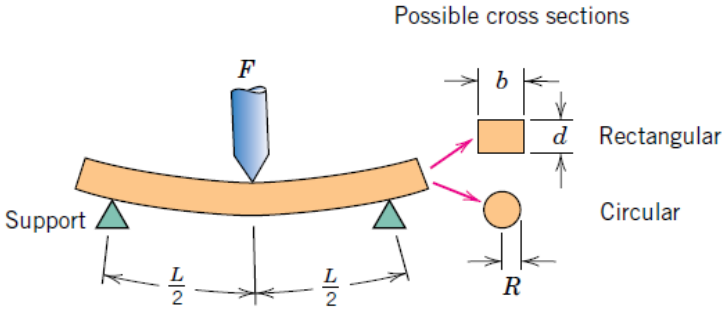

Figure 7*: Three-point bending scheme [1]*

2.3 Production Output Equation Derivation

Considering that the goal of the project is optimizing the copper wore production, which includes maximizing the output, finding an equation of machine's daily output is a vital component for optimizing the whole production process. Daily output of the machine is strongly dependent on the casting speed, the pull distance and the interval time. Hence it is possible to derive the equation relative to these parameters.

First of all, to approximate the daily output one should calculate the time required for the machine to complete the single withdrawal cycle described in ***Figure 4***. Denoting the casting speed as *v*, pull distance as *d*, interval time as τ, and *t* as the time to complete a single pull, the time required for the machine to complete a single withdrawal cycle will be given as:

$$t_{cycle} = \tau + t \tag{2.5}$$

where $t = \frac{d}{v}$

From the equation (2.5) and a constant 7 hour working shift, we can determine the number of cycles *N*, which the machine will make in a single working shift, which will be given as:

$$N = \frac{T}{\tau + t} = \frac{7 * 3600}{\tau + t} = \frac{25200}{\tau + t} \tag{2.6}$$

From equation (2.6) we can obtain the daily production capacity equation in terms of volume of copper rod for the casting machine by:

$$V = \frac{TdA}{\tau + t} = \frac{TdA}{\tau + \frac{d}{v}} = \frac{TdAv}{d + \tau v} \tag{2.7}$$

From the equation (2.7), it is now possible to calculate the daily production capacity of copper rod in terms of mass in kilograms using the formula (2.8), where m is the mass of copper rod produced daily, and ρ is the density of copper rod.

$$m = \rho V \tag{2.8}$$

In order to optimize the production of copper rod to reach acceptable quality/quantity ratio, the agenda is to optimize the equation (2.7) which controls the maximum output of the machine.

Chapter 3: Results and Discussion

3.1 Sample Casting Process

Casting process was conducted according to the setup described in Chapter 2.1 and 2.2. The main aspects of the experiment were copper cathode scrap smelting and degassing process, adding the constant superheat modulus and casting of the specimen according to parameter sets described in ***Table 1.***

3.1.1 Metal Melting and Casting Procedure

The casting process begins with setting up the water pump and water chiller which are used to cool the inductor coil and the heat exchanger. The water chiller unit was set to maintain the water temperature at a constant value of 25°C. Furthermore, the water flow rate was held at a constant 25 liters per minute using a 370 W/h water pump. Pure copper cathode used in the cable manufacturing industry was placed in the SiC crucible with a total capacity of 100kg and the electromagnetic induction heating unit was turned on and set to the melting point of copper at 1085°C. Upon reaching the melting point of copper and having a uniform copper liquid, it could be noticed that the surface of the copper melt was releasing internal gases. Since it is impossible to start the casting process while the gas is being released from the melt, graphite flake was added to cover the whole surface area of the melt. The reaction between the graphite and copper melt along with the electromagnetic melt steering feature of the machine results in release of most of the gases present in the melt. After 40 minutes no noticeable gas release from the melt was recorded, hence the experiment proceeded with the casting process. The heat exchanger with the graphite mold for casting copper rod was submerged to the copper melt and the withdrawal unit was enabled to start the casting process. The casting speed, pull distance and interval time were gradually changed according to ***Table 1*** to prepare the initial specimen which were subject to further investigation using XRD and mechanical testing.

3.1.2 Casting Results and Sample Preparation

Samples were initially retrieved from the rod winding machine and cut to equal length specimens of 2 meters except for specimen 8 for which the casting process failed shortly after

setup of the parameters. Observation of the specimen showed that it underwent insufficient solidification process resulting in discontinuation of the cast rod. Additionally, noticeable visual differences were observed for all 10 specimens. More specifically, all specimen were covered in a thin copper oxide layer. For each case the oxide layer thickness and color were different, which most likely indicates the differences in solidification and cooling process in the graphite mold and the heat exchanger respectively. The differences in the oxide layer of cast rods can be observed in ***Figure 8***. The specimens are depicted in the ascending order, from left to right.

Figure 8*: Copper rods cast in the scope of experiment (left to right specimen 1 to 10)*

The initial guess for the study was that the darker specimen underwent incomplete cooling process, since the dark color is noticeable in the specimen with high casting speeds, high pull distance and low interval time. It can be deduced that the oxide layer thickness is related to the rod temperature at the outlet of the machine. It could also be noticed that the specimen with severe surface oxidation were also harder to bend rather than those with brighter colors, but this was to be further investigated through the mechanical testing.

The next step of the study was the preparation of the copper rod specimen for XRD test. After discussions with the staff from Chemical Physics Institute of Yerevan it was decided to prepare specimen with 10mm length from the initial samples gathered during the casting process. Then the specimens were cut in longitude in the prototyping lab of American University of

Armenia (AUA), using CNC machinery. Samples were then handed to the Chemical Physics Institute for XRD test.

Mechanical testing of the specimen was conducted in the mechanics lab of AUA. The in-house built three point bending setup can be seen in ***Figure 9.*** As mentioned in the previous chapter, the length of the specimens were taken 230 mm and the radius was 3.75 mm. A load of 1.1 kg was applied on all 10 specimens, to determine the dependence of flexural strength of the rods on the casting parameter change. The displacement under the load, along with the other variables was plugged in the equation (2.4) to determine the flexural strength of the rods. This is not an exact measurement, as we technically need to do number of measurements and take the slope of the stress-strain curve as the flexural modulus, but in part due to technical limitations we have limited ourselves to just one experiment. Another reason for this is that we have somewhat wide tolerance for error, and it is the overall flexural modulus trend that is important for us.

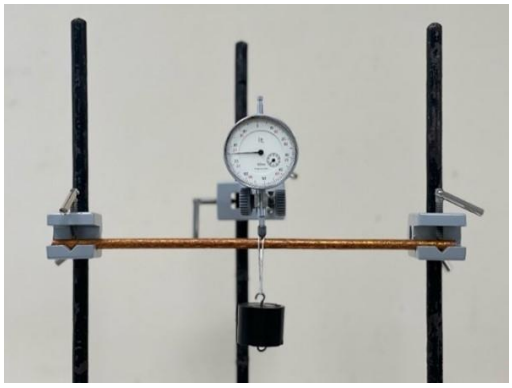

Figure 9*: Experimental Setup for the three-point bending test*

3.2 XRD Results Discussion

Average crystallite size for each specimen were calculated using equation (2.1). Furthermore, the interplanar spacing of the diffraction pattern and the lattice constants of the experimental films were evaluated using equations (2.2) and (2.3) respectively. ***Figure 10*** depicts an example of actual peaks found in all 10 copper wires tested. While there is some slight variation in the peaks between various samples, the variation is not significant enough to include all 10 samples, or to have a more detailed discussion. Five distinct peaks were observed in all samples at around 43.8°, 50.8°, 74.5°, 90.2°, 95.5°. These peaks are routinely found in copper [14], and

correspond to (111), (200) and (220), (311) and (222) crystallographic planes of copper FCC crystal structure. Furthermore, in all of the samples (111) and (200) planes were found to be the most dominant planes, which is a confirmation of other reports [14]. It is well known [10] that in FCC structures, the Miller indices h, k, and l must be either all odd or all even. Only finding these five peaks are also an indication of the purity of the produced rods. While the surface of the samples was treated to remove the copper oxide layer that we saw in ***Figure 8***, no further impurities on or inside the copper rod was observed. As discussed in the Chapter 2, the average crystallite sizes for the rods were estimated using the Scherrer equation (2.1), and the results were plotted. The results of the parameter change on the crystallite size of specimen is shown in ***Figure 11.*** As it can be seen, while no substantial variation of the crystal size was observed, the most significant effect on the average crystal size is due to variation of casting speed and interval time, whereas the pull distance has only a minor effect. Furthermore, it can be seen that casting speed has negative correlation in regards of crystallite size, while interval time and pull distance have positive correlation. It can be deduced from the plots that nucleation process inside the graphite mold is somewhat dependent on the casting parameters. Having five peaks of considerable intensity is a definite proof of highly polycrystalline nature of the copper rod, which also means a significant number of boundaries that is expected to affect the mechanical properties of the samples. Meyersm and Ashworth [15] explain that the incompatibility between differently oriented grains results in significant grain boundary stresses when the sample is under loading. This interboundary stress can be significantly larger than the bulk stress of the sample, hence a plastic deformation in the grain boundary region initiates much earlier than in the bulk sample. Considering that copper undergoes work hardening, larger hardness for samples with smaller crystal sizes is expected.

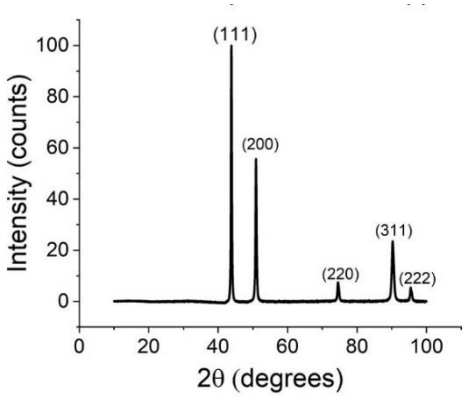

Figure 10*: XRD diffraction peaks of the copper wire*

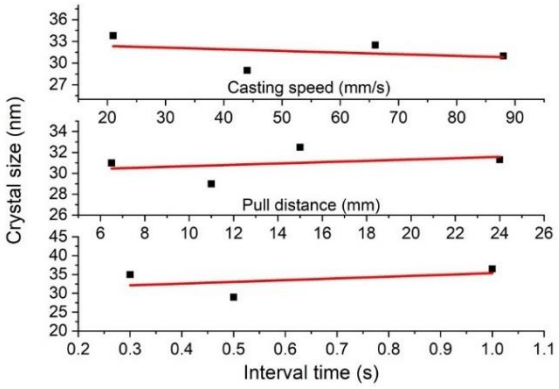

Figure 11*: Average crystal size vs various parameters*

3.3 Mechanical Property Test Result Discussion

Three point bending test revealed strong dependance of flexural strength on casting speed, pull distance and interval time parameter changes. ***Figure 12*** shows the results of the three-point bending test on all 10 specimens.

As it can be seen, all three parameters significantly affect the Young's modulus of the samples. Furthermore, the Young's modulus dependence on the parameter changes is somewhat different between the parameters. The only parameter that has a negative trend was found to be the interval time, where the Young's modulus decreases following an exponential-like function. This is in-line with our predictions in the previous section. Smaller crystal sizes for small interval times should result in larger strength. Another explanation for this behavior is that low interval time means the rod is still warm when it is pulled, hence it undergoes even more work hardening. It is worth mentioning, that at the lowest interval time of 0.1 s, the experiment was unsuccessful, as the casting is too fast and the rod fails. This means that interval times of 0.3-1 s should be chosen, where we do not see too much variation, which suggests that the effect of interval time on the Young's modulus is limited to too short interval times and is mostly absent for larger interval times.

There is a linear upward dependence of Young's modulus on casting speed, and the slope of the line is relatively steep, resulting in extremely high Young's modulus of around 350 MPa – the highest values among all samples. This trend again matches our prediction based on the average crystalline size behavior. It can also be further explained using the same logic as the interval time, i.e. faster casting means more work hardening. Considering the linear trend observed, the casting speed has to be limited in order to have a Young's modulus low enough to make wire drawing possible.

The most unexpected behavior was observed for the experiments where the pull distance was varied. While the crystalline size dependent prediction was suggesting a downward trend, we see an upward trend for the Young's modulus. Further analyses are required to give a compelling explanation, however, with increasing pull distance, we should again see more work hardening, which should be one of the main reasons why we see an upward trend. It should also be noted, that

after the initial steep rise, the Young's modulus curve reaches a plateau at around 255 MPa after pull distance of 11mm, meaning a favorable behavior for maximizing the production output.

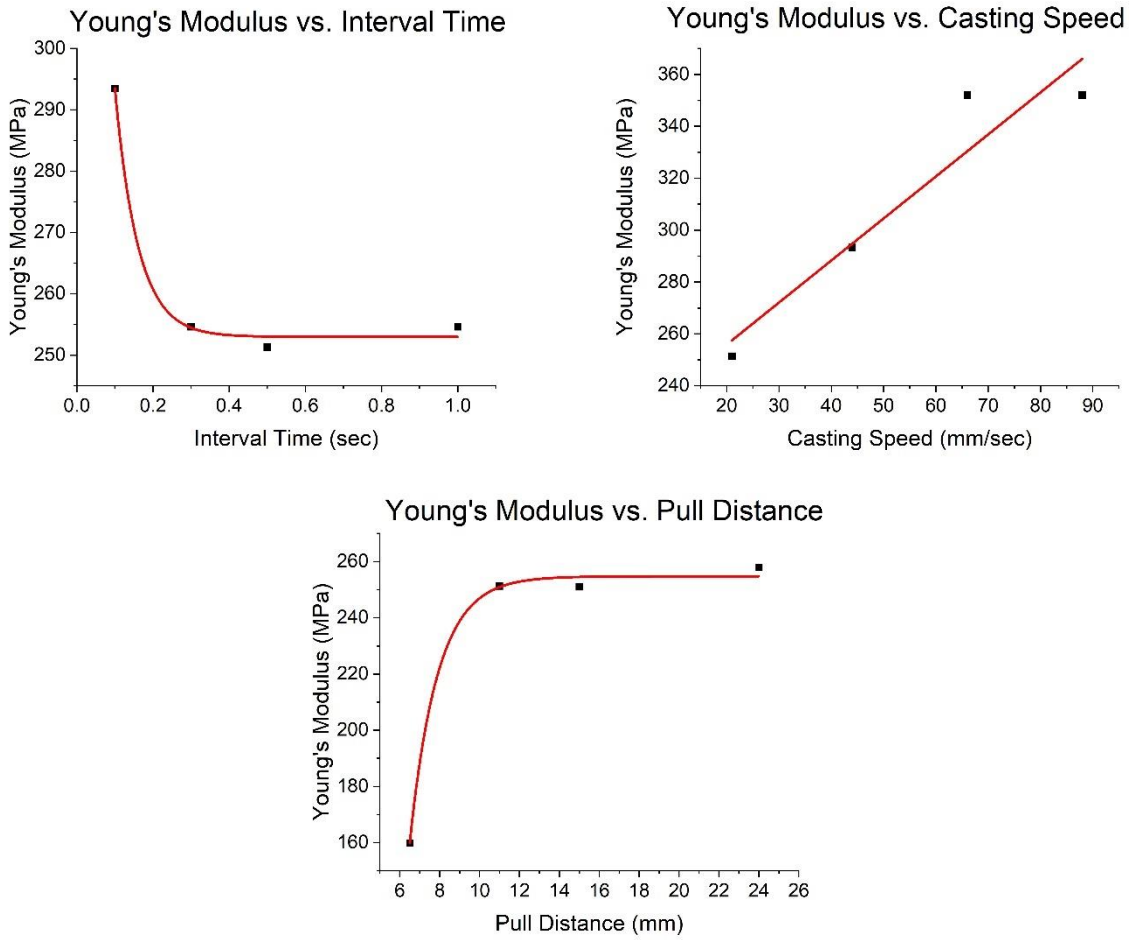

***Figure 12**: Variation of Young's Modulus of prepared samples as a function of casting parameters*

To further analyze the dependence of the Young's modulus on casting parameters, and optimize these parameters for the commercial production, it is important to quantify the variations of the Young's modulus with respect to casting parameters. A simple single function fitting was performed on the data shown in ***Figure 12*** using OriginPro (© OriginLab Corporation). Corresponding function approximations for each of the above cases can be estimated where E is the Young's modulus in MPa, v is the casting speed in mm/sec, d is the pull distance in mm and τ is the interval time in seconds. Hence, for each case the functions are the following:

For casting speed

$$E_1 = 223.5 + 1.62 * v \tag{3.1}$$

For pull distance

$$E_2 = 242.8 * (d - 6.5)^{0.02} \tag{3.2}$$

For interval time

$$E_3 = 253 + 211.5 * e^{-16.5*\tau} \tag{3.3}$$

Here, the notation E_1, E_2, E_3 is for convenience.

One issue that is present with the above results, is that it is based on limited number of experiments, hence further experiments are needed to verify and improve if needed.

3.4 Multi-Objective Optimization of the Production

Since the final goal of this project is to maximize the production output of the Upward Continuous Casting process, and there are three variables affecting the properties from one side and the output from another, it is vital to solve a multi-objective optimization problem with certain constraints, to find the most optimal production parameters for the machine. As discussed earlier in Chapter 2 the production volume can be estimated using the equation (2.7):

$$V = \frac{T * d * A * v}{d + \tau * v}$$

where V is the produced volume, T is the shift time, d is the pull distance, A is the cross-sectional area of the conductor, v is the casting speed and τ is the interval time. In the (2.7) equation, ignoring T will mean V is per unit time. Also, A is fixed, hence we can ignore it too, thus V will become per unit area as well.

As we see from equation (2.7), in order to maximize V, we need to minimize τ, or maximize d and v. However, as we saw from ***Figure 12***, and discussed in the previous chapter, lowering τ, as well

increasing *d* and *v* increases the Young's modulus which should also be taken into account, as we may produce rods that are too stiff for wire drawing.

As we see from the equations (3.1) - (3.3), finding the optimal τ, *v* and *d* values is not trivial, especially considering the non-linearity of the equations. Finding the optimal parameters may be viewed as a multi-objective optimization problem. Multi-objective optimization is used when there is a need to find optimal values for two or more functions (usually referred as objective functions) that require some trade-off between the two conflicting functions. A multi-objective optimization problem, where we want to minimize the functions can be described as:

$$f = \text{argmin}(f_1 + \lambda * f_2) \tag{3.4}$$

which may be subject to number of constraints. Eq. (3.4) needs to be solved for a large range of λ values and an f_1 vs. f_2 plot – called a Pareto front has to be constructed, as shown in ***Figure 13***. The points on the curve for which neither objective function can be decreased without increasing the other one is called the "knee point" or the optimal Pareto front. All points on the curve are solutions, however, an optimal trade-off point will be when the slope of the curve is steep.

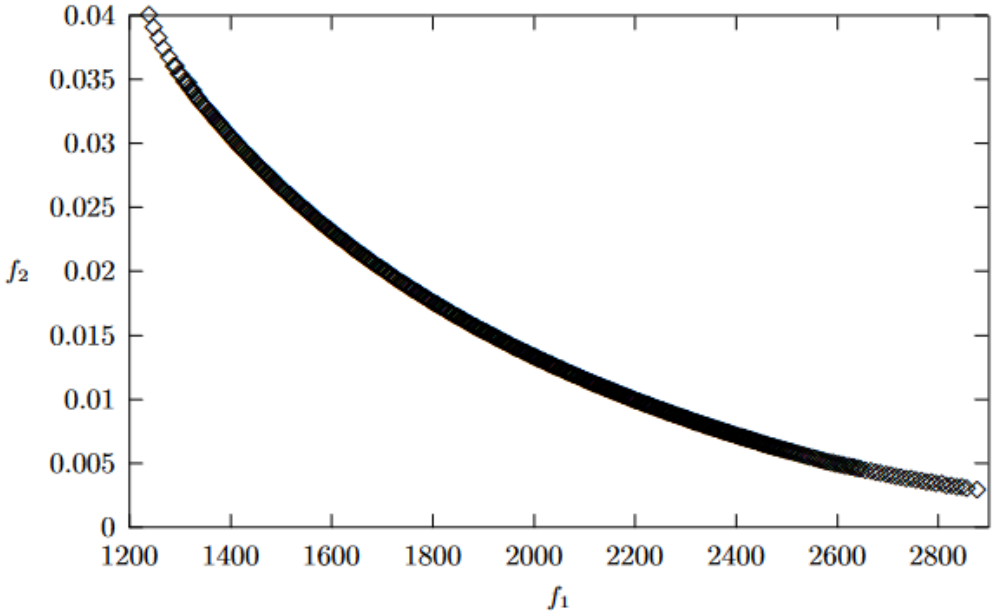

***Figure 13**: Pareto front for two objective functions f_1 and f_2 [11]*

In our case, we have three parameters - τ, *v* and *d*, and three objective functions:

$$f_1 = \frac{1}{V} = \frac{x_1 + x_2 * x_3}{x_1 * x_3}$$

$$f_2 = 242.8 * (x_1 - 6.5)^{0.02} \tag{3.5}$$

$$f_3 = 253 + 211.5 * e^{-16.5 * x_2}$$

$$f_4 = 223.5 + 1.62 * x_3$$

where $x_1=d$, $x_2=\tau$, $x_3=v$. f_1 is the inverse of the volume produced V, since we want to maximize V, hence minimize the reciprocal of it. Usually, multi-objective optimization is subject to certain constraints for the variables. In our case, those constraints are the physical limitations of the apparatus:

$$\begin{gathered} 6.5 \leq x_1 \leq 24 \\ 0.1 \leq x_2 \leq 1 \\ 21 \leq x_3 \leq 88 \end{gathered} \tag{3.6}$$

High Young's modulus means that the wire-drawing process will be difficult, and at too high values even impossible, hence another constraint, based on the experience, was placed on Young's modulus as:

$$E \leq 270 \text{ MPa} \tag{3.7}$$

Furthermore, since it is known that the casting process failed for the value of $\tau = 0.1$s it was decided to update the constraints to values which are experimentally viable. Hence our final constraints for the estimations are described as

$$\begin{gathered} 6.5 \leq x_1 \leq 24 \\ 0.3 \leq x_2 \leq 1 \end{gathered} \tag{3.8}$$

$$21 \leq x_3 \leq 88$$

In order to solve the given multi-objective optimization problem, we have modified a multi-objective optimization code (see Appendix A) from literature [12]. It is worth mentioning, that an optimization problem as complicated as the one in (3.5) requires too much computational power and too many points to converge to a good estimation. Also, the fitting equation (3.1) – (3.3) are based on limited number of experimental data, hence there is a good chance that there is some inaccuracy in the values. An example of a Pareto front for optimization problem (3.5) subject to (3.7) and (3.8) constraints and for 5000 points is given in ***Figure 14.***

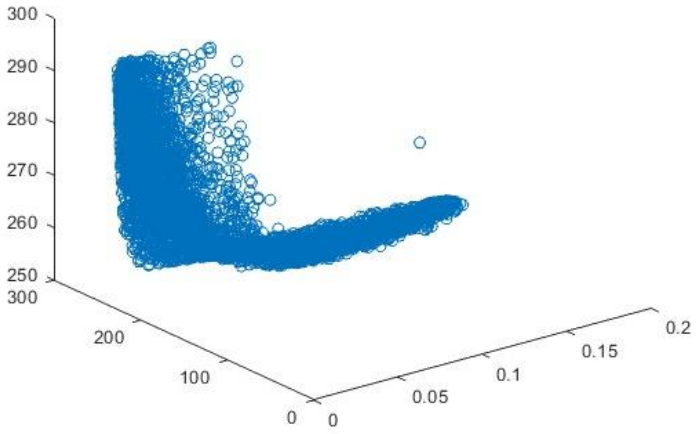

Figure 14*: The multi-dimensional Pareto front of eq. (3.5)*

By solving the optimization problem, we found that the optimal values, that will maximize production, and keep the Young's modulus below 270 MPa are d = 24 mm, τ = 0.35 s, v = 28,5 mm/s. For these values, the volume of production will be 20 mm per second and around 504 meters daily. Plugging in the values to the equation (2.8) shows that the daily output would be m = 224 kg for a single casting head. Since the machine is equipped with two casting heads (meaning it cast two separate rods simultaneously), the theoretical maximum daily output of the machine can reach up to 448kg.

Chapter 4: Conclusions and Future Work

Copper rod samples were fabricated in a wide range of casting speeds, pull distances and interval times. XRD analyses was performed to verify the crystalline structure of the copper rods, and it was found that there is some variation in the average crystal sizes, which had a slight increase with increasing pull distance and interval time, and a slight decrease with increasing casting speed. Mechanical analysis demonstrated that variation of casting parameters has a significant effect on the properties of the copper rods. It was found that there is a significant visual difference between the samples, which can already be a loose indicator of the properties. Samples that correspond to large pull distances were found to be of a darker color, as there was an intensive layer of oxide on the surface. It was also found that these samples had too high Young's modulus to be a successful candidate for wire drawing process. Besides, the Young's modulus was found to increase with increasing casting speed and decreasing interval times. Considering the goal of the project is maximizing the production output, and the three parameters to maximize the production output increase the Young's modulus, a multi-objective optimization problem was solved to find the optimal parameters. It was found that the optimal parameters are d = 24 mm, τ = 0.35 s, v = 28,5 mm/s, which were reported to the production manager of 'N-S' LLC, and shortly the mass production of copper rod using the above parameters will be arranged.

Due to technical and financial limitations, only limited number of experiments were conducted. To improve the results and lower the error, it is critical to have significantly larger number of experiments. Furthermore, the mechanical testing was done on an in-house built testing setup with limited capabilities. Using a better apparatus could improve the results. Furthermore, the mass production scale wire drawing procedure will reveal the actual results of the current study, and possible changes might take place to improve the production quality.

References

[1] Callister, William D., and David G. Rethwisch. Materials Science and Engineering. Hoboken, NJ: Wiley, 2020.

[2] Maina, Martin Ruthandi, and Yasuhiro Okamoto. Physical Properties of Copper. n.d. https://www.researchgate.net/figure/Physical-properties-of-copper-C1020_tbl1_329159652.

[3] Grigoryan, A. (2011) 2011. Технология производства кабелей и проводов. Edited by I. Peshkov. Машиностроение.

[4] “Описание Параметра ‘Класс Гибкости Жил.’” Описание параметра "Класс гибкости жил" - Профсектор. Accessed October 7, 2022. https://profsector.com/parameter/1236/klass-ghibkosti-zhil.

[5] “Power Cables: High, Medium and Low Voltage Power Cables.” Power Cables and Wires. Accessed October 17, 2022. https://www.alfanar.com/HV-power-cables.

[6] “Technologies of Continuous Casting: Horizontal, Vertical Downward, Vertical Upward.” KMM. Accessed October 18, 2022. https://kmmbronze.com/technologies-of-continuous-casting-horizontal-vertical-downward-vertical-upward/. [1]

[7] Härkki, K., and J. Miettinen. “Mathematical Modeling of Copper and Brass Upcasting.” Metallurgical and Materials Transactions B 30, no. 1 (1999): 75–98. https://doi.org/10.1007/s11663-999-0009-6.

[8] International Electrotechnical Commission. “Conductors of Insulated Cables, IEC60228” November 2004.

[9] Richardson, H. Wayne. Handbook of Copper Compounds and Applications. New York: Marcel Dekker, 1997.

[10] B. D. Cullity, S. R. Stock, Elements of X-Ray Diffraction (3rd Edition), Prentice-hall, New Jersey, 2001

[11] Teich, J. (2001, July). Pareto-front exploration with uncertain objectives. In Evolutionary Multi-Criterion Optimization: First International Conference, EMO 2001 Zurich, Switzerland, March 7–9, 2001
Proceedings (pp. 314-328). Berlin, Heidelberg: Springer Berlin Heidelberg.

[12] Son Duy Dao. How to Solve Triple-Objective Optimization Problems Using Matlab, October 31, 2020, Retrieved from https://learnwithpanda.com/2020/10/31/how-to-solve-triple-objective-optimization-problems-using-matlab/, Retrieved on May 8, 2023

[13] Merz, M. D., & Dahlgren, S. D. (1975). Tensile strength and work hardening of ultrafine-grained high-purity copper. Journal of Applied Physics, 46(8), 3235-3237.

[14] Thakar, M. A., Jha, S. S., Phasinam, K., Manne, R., Qureshi, Y., & Babu, V. H. (2022). X ray diffraction (XRD) analysis and evaluation of antioxidant activity of copper oxide nanoparticles synthesized from leaf extract of Cissus vitiginea. Materials Today: Proceedings, 51, 319-324.

[15] Meyersm, M. A., & Ashworth, E. (1982). A model for the effect of grain size on the yield stress of metals. Philosophical Magazine A, 46(5), 737-759.